Energy Conversion and Management: X 12 (2021) 100120

Contents lists available at ScienceDirect

Energy Conversion and Management: X

journal homepage: www.sciencedirect.com/journal/energy-conversion-and-management-x

Performance optimization of a dual-rotor ducted wind turbine by using response surface method

Javad Taghinezhad [a,*], Reza Alimardani [a], Mehran Masdari [b], Esmail Mahmoodi [c]

[a] Department of Biosystem Engineering, Faculty of Engineering & Technology, University of Tehran, Iran
[b] Faculty of New Science and Technology, University of Tehran, Tehran, Iran
[c] Department of Mechanical Engineering of Biosystems, Shahrood University of Technology, Shahrood, Iran

ARTICLE INFO

Keyword:
Ducted wind turbine
Dual rotor wind turbine
Optimization
Response surface methodology
Central composite design

ABSTRACT

The presented study evaluates and optimizes the performance of dual-rotor wind turbines installed inside a developed duct. The effect of different operating conditions on the extracted power was compared between dual-rotor wind turbines (DRWT) and single rotor wind turbines (SRWT). These operating conditions include the type of dual-rotor wind turbines installed in the throat section of the duct, the distance between the two rotors of a turbine, and the flow velocity through the duct throat that were evaluated by the multivariate statistical method response surface methodology. The central composite design of the response surface method was utilized to fit the designed model based on the least-squares method. Also, the multiple regression method was applied for the empirical data to match variable operating conditions with the developed model by analysis of variance (ANOVA). Afterward, some experiments were carried on to validate this method. The results showed a maximum power ratio of about 55% at the optimized conditions for dual rotor wind turbines. Determined P-values for designed parameters of models were less than 0.05, which makes its effect on the model significant. Furthermore, the power ratio obtained from empirical data was compatible with the considered model.

1. Introduction

The present energy system is heavily dependent on fossil fuels, although changes in political and social conditions have accelerated renewable energy growth in recent decades. Wind energy is a type of renewable energy with huge reserves and distribution worldwide. Consequently, the optimum performance design of wind turbines for the utilization of renewable energy is essential for the 21st century. However, wind power is far from its full potential. In the last two decades, conventional wind turbines have developed continuously. This improvement led to constructing large turbines with larger blades and taller towers, increasing production and maintenance costs. Also, electrical transmission is another cost of these turbines.

In recent years, research on ducted wind turbines for small effective wind applications has been studied as an economical method. Various researchers have tried to increase the efficiency and performance of this type of turbine. Allaei [1–3] Introduced a kind of ducted wind turbine called INVELOX, which used a flow collector and a venturi-shaped cross-section to convert wind energy into electricity. Their studies mainly focused on the structure and modeling of ducts. One of their studies investigated the effect of using two/three turbines in the duct throat section experimentally [4]. Gavade [5] introduced a new concept of wind harnessing to produce power at a lower cost. They reported wind velocity at the venturi section increased two times while 6 m/s in the inlet section. Some researchers worldwide have developed inventions [3–4,6–8] that demonstrate specific applications in wind power generation. For example, Air Born wind turbines were designed with turbines 300–500 m above the ground. Various types of ducted, single-ducted, and multi-ducted turbines have been developed [6,8–10].

Most wind turbines utilize an SRWT design, with three blades rotor placed onto a hub at the front of a turbine tower, as conventional, ducted, air born, and Invelox kinds [11]. Many efforts have been made to improve single-rotor wind turbines' performance by researching the blade design, increasing rotor and tower sizes to achieve higher wind speeds at higher altitudes. Large rotors also cause several problems, such as blade surface pressures, vibration loads, loading noise due to aerodynamic and gravitational loads, and require ample space and strong wind to operate.

The concept of DRWTs was created and developed by researchers to supply low-cost energy and increase wind turbines' output power from a fixed swept area. In DRWT's, two rotors are placed in a row and back to

* Corresponding author.
E-mail address: j.taghinezhad@ut.ac.ir (J. Taghinezhad).

https://doi.org/10.1016/j.ecmx.2021.100120
Received 26 July 2021; Received in revised form 2 October 2021; Accepted 16 October 2021
Available online 20 October 2021

Nomenclature

α	Torsion angle of the airfoil (deg)
A	Wind speed in duct throat (m/s)
B	Distance ratio
c	Local chord length (m)
C	Turbine type
CO	Co-rotating
CR	Counter-rotating
D_t	Duct throat diameter (m)
m	Meter
mm	Millimeter
n	Quantity of factors
n_c	Quantity of replications
n_t	Quantity of categorical factors
N	Quantity of experiments runs
r	Local turbine radius (m)
R	Turbine Radius (m)
R^2	Coefficient of determination
U_0	Inlet wind speed (m/s)
X_n	Independent variables
Y	Response of experiment
ANOVA	Analysis of variance
ABL	Atmospheric Boundary Layer
CCD	Central composite design
DRWT	Dual-rotor wind turbines
RSM	Responsive surface method
SRWT	Single rotor wind turbines

back, which increases the energy extraction capacity from a fixed swept area. Some researchers have studied numerical and experimental methods to compare DRWTs with SRWTs and reported an increase in harvested wind energy compared to SRWT's. Khalefa [12] shown that in wind turbines performance, the most considerable correlation is between power and wind speed,with this regard, ducted wind turbines focus on increasing wind speed, so using DRWT's in the ducts can be considered a new challenge.

When there is a variable interaction, the traditional approach will be highly time-consuming and difficult to identify the optimum conditions. The classical form may lead to uncertainty, incorrect results, and the need to spend time and work. Also, it does not guarantee optimal conditions and cannot determine the interaction between two or more factors. As a helpful method, the Responsive Surface Method (RSM) is a statistical approach that analyzes equations by providing a minimum number of experiments for many determinants and multivariate [13]. RSM is a set of statistical techniques and applied mathematics for designing experimental models. RSM is a powerful optimization tool introduced by Box and Wilson in 1951 [14], a statistical package and mathematical technique for developing, improving, and optimizing various processes. This method can effectively evaluate the effect of multiple factors and their interaction on different interaction levels and is often used for multi-level optimization methods, optimal conditions, and their relationship analysis. In this method, fewer treatments and less time are required than conventional methods to obtain maximum efficiency and reliability of test accuracy [15].

RSM is widely used to optimize wind energy systems, such as wind energy recovery of wind turbines [16], the performance of Invelox wind turbine diffusers [9], the parameters of the controllers used in the frequency converter of a variable speed wind turbine [17], estimating site-specific wind turbine loads in ultimate and fatigue limit state [18]. The goal of the presented study is to optimize the distance between two rotors of dual rotors wind turbines installed in the throat section of a duct,with this regard, the size of the rotors has a significant effect on the performance of ducted wind turbines or not. Up to now, no analysis has been done on ducted wind turbines to study the impact of distance between two rotors on output power using the RSM approach. The main part of this study was to develop, fabricate, and evaluate four types of DRWT located in a developed duct. First of all, blades, rotors, and turbines are designed and fabricated then the turbines are installed inside the throat section of a duct. Finally, the performance of the designed ducted wind turbines was evaluated experimentally. The main goal of this work was to estimate the best distance between two rotors of a DRWT's in ducted wind turbines.

2. Material and method

2.1. Specifications for rotor and blade of turbines

The first step in designing the wind turbine blade is selecting the suitable airfoil to use an airfoil with a high lift-to-drag ratio. Also, due to the small size of the turbines, the designed blades must have the necessary strength against high wind speed. Therefore, NACA 4424 airfoil was used to prepare the blades [19]. Depending on the

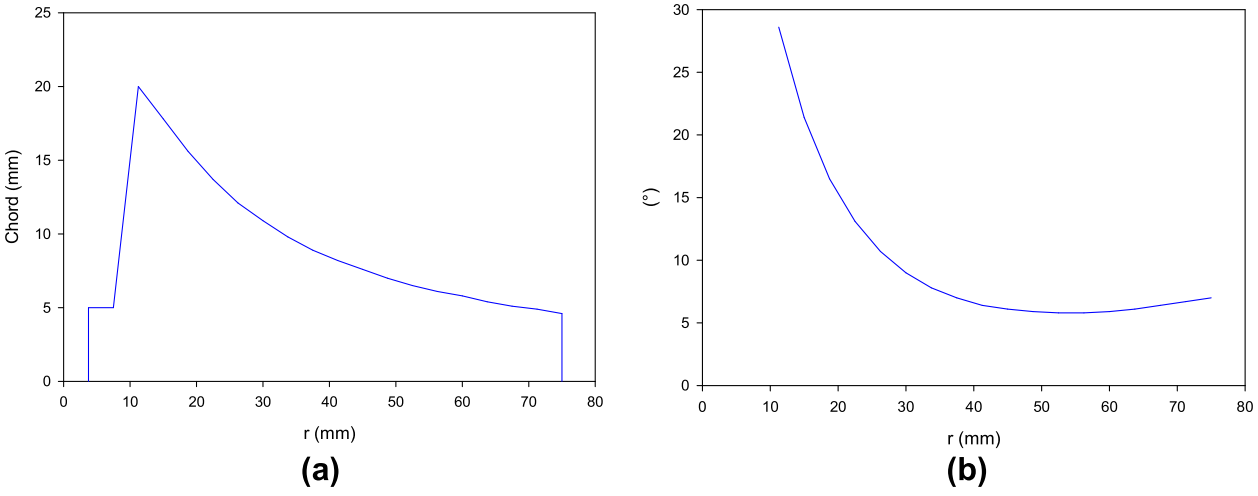

Fig. 1. Chord length diagram for the blade modeled along with the blade length (a), Pitch angle diagram for blade modeled along the blade (b).

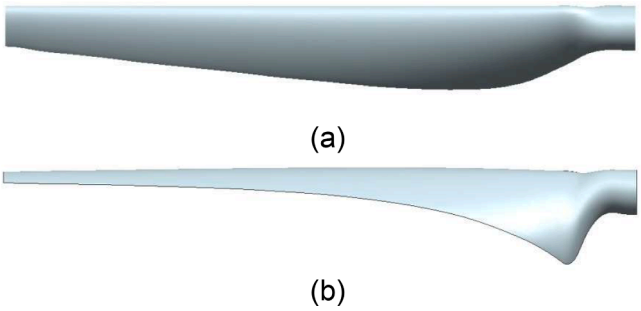

Fig. 2. Modeled blade top or side view (a) front view (b) of the flow.

dimensions of the duct throat section (turbine installation location), a three blades horizontal wind turbine with a diameter of 0.15 m for a larger turbine and a smaller turbine with half-scale of a large turbine was considered for experimental tests and then blade, hub and Other components of the wind turbine designed. The chord length and pitch angle along the blade for this airfoil are shown in Fig. 1. The chord length at the blade's tip is about 5 mm, and its maximum value along the blades is 20 mm.

The modeled blade in NX 10.0 software is shown in Fig. 2. Table A1 presents the chord length and torsion angle as a function of the blade radius. Using this information, all the details of the blade geometry are available.

Table 1
Specification of rotors used for study distance effect of rotors.

Specification	Front Rotor	Rear Rotor
Number of Blades	3	3
Rotor Diameter	75 mm/ 150 mm	150 mm
Rotor Position	Upwind	Upwind
Airfoil Type	NACA 4424	NACA 4424
Blade Material	ABS	ABS
Rotation	Counter/ Clockwise	Clockwise

2.2. Study the distance between two rotors

To investigate the impact of rotors' distance on turbine output power variables defined as independent and dependent. The independent variables are wind speed and relative axial length. Wind speed is limited in three levels of 10 m/s (low rate), 14 m/s (medium rate), and 20 m/s (high rate) and relative axial distance (ratio between the axial length of two rotors to the duct throat diameter) 0.25; 0.45 and 0.65. The dependent variable is the angular velocity of the shaft and output power generated from the front rotor and rear rotor.

Specification of rotors used in experimental tests is shown in Table 1. The front rotor has a diameter of 75 mm on the study object, while the rear rotor has a diameter of 150 mm, as shown in Fig. 3. The front rotor rotates in the clockwise direction, and the rear rotor rotates in the opposite direction; in other means, two rotors rotate in a counter-rotating position. Each rotor is supported by a solid shaft on a separate DC motor. Both rotors are placed in the ducts' throat section and can move on the horizontal axis and be fixed at a defined distance.

The duct used in this research was designed and fabricated by Taghinezhad [20] based on the methods used by researchers for creating different wind tunnel parts. The duct model was designed in three sections for ducted wind turbine systems and is presented in Fig. 4,the inlet section was developed based on Morel's [21,22] proposed technique. The throat region was supposed to be the main place to put the wind turbine. The discharge section is considered to recover the wake flow consequence from the throat section and releasing flow to the free stream.

The electrical power generated by the DC motors can be calculated by measuring the output voltage of the V_T multiple the measured current I_L [23]. The total generated power is the sum of the power in the rear and front rotors.

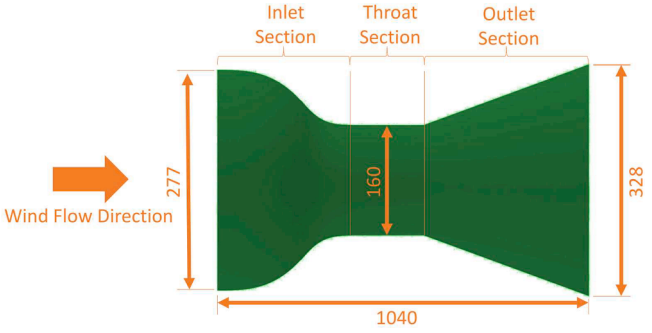

Fig. 4. Overall Structure of the ducted wind turbine systems (Dimensions are in mm).

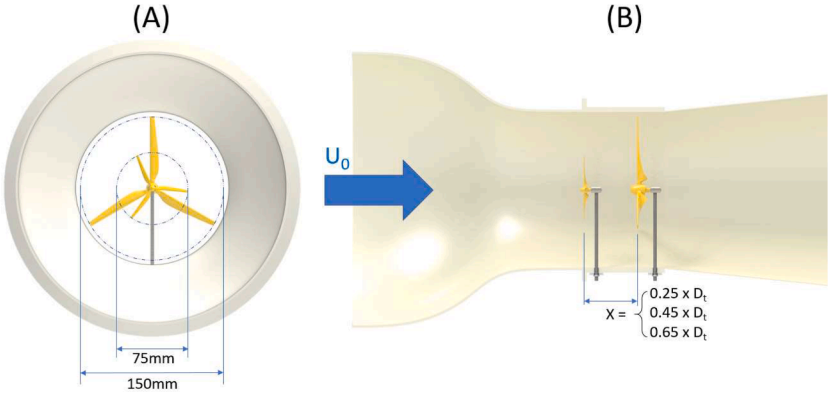

Fig. 3. Installation of rotors inside of duct (A) Front View (B) Section View and applied variables.

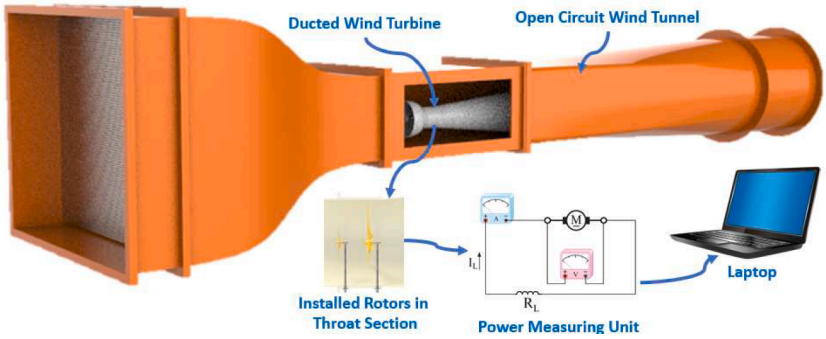

Fig. 5. Arrangement of the experimental setup to measure the turbines output power.

2.3. Investigation of rotation direction on output power

Three types of turbines with a different arrangement of rotors were selected to study the effect of rotors rotating direction on turbine output power. A small rotor in front of a big rotor (SB), a big rotor in front of a big rotor (BB), and a big rotor in front of a small rotor (BS) were arranged to study in experimental tests; rotors can rotate clockwise or counterclockwise. Wind speed is defined in seven levels from 4 m/s to 16 m/s by increasing 2 m/s in each data collection step.

2.4. Examination method

All experiments in this research were conducted in the wind tunnel of the Experimental Aerodynamics Laboratory of the University of Tehran, Faculty of New Sciences and Technologies. It is an open-circuit wind tunnel with the capacity of generating a maximum Atmospheric Boundary Layer (ABL) wind speed of 45 m/s. This wind tunnel is a suction type that includes a bell-shaped inlet, a relaxation chamber with mesh layers, nozzle, test chamber, diffuser, and axial fan (Fig. 5. The total length of the tunnel circuit is 12.5 m, and the length of the test section is 1.5 m. Also, its width and height are 1 and 0.7 m, respectively. The turbulence intensity of the wind tunnel in the test section was measured at 0.4% on average.

As shown in Figs. 3 and 5, the developed duct was installed in the wind tunnel's test section, while rotors were located in the throat section of the duct. Each rotor's output voltage and current were measured during the experimental test, and collected data were transferred to a laptop for analysis. Blockage ratio was measured for installed setup as 11.4% in test section then the blockage did not affect the results of tests [24].

2.5. Design of experiment

Standard RSM analyzed the performance of different types of DRWTs. RSM presents statistical and mathematical methods generated from experimental models to fit the empirical data related to the experimental setup. It is used to optimize the designed factors by minimizing the number of runs in the experiment and studying the interaction between the factors [25]. The study of optimization in RSM can be divided into six stages [26]:

(1) We are selecting variables independent with significant effects on the system by determining the limits of the experiment.
(2) Design of experiment and perform the experiments accordingly.
(3) Statistical-mathematical analysis of experimental data obtained through a suitable polynomial function
(4) Evaluation of model fit (p-value, R squared, Graphs, etc.)
(5) Confirmation of necessity and possibility of making a change in the direction of desired area (if one side of the range is optimized)

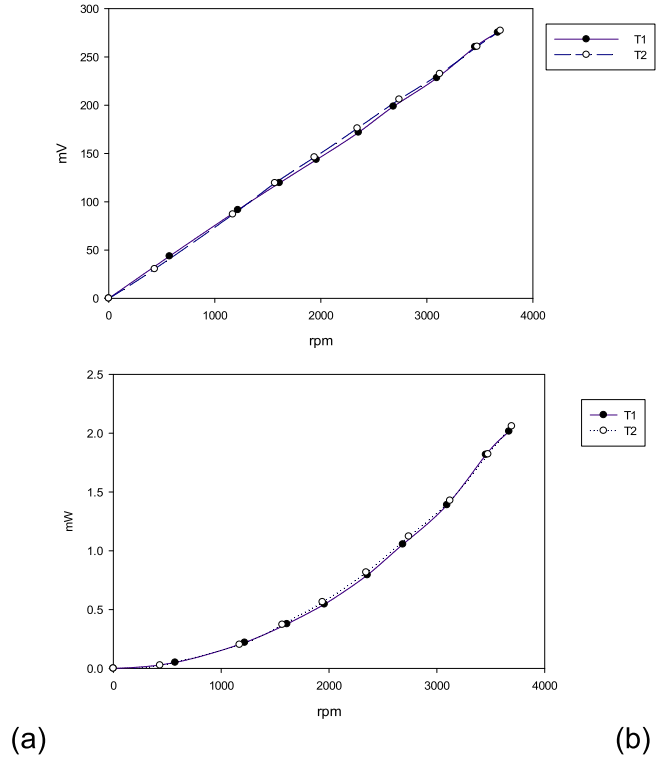

Fig. 6. Output voltage (a) and power (b) for two DC motors used in tests in the same condition.

(6) Obtain optimal values for each variable

In this study, three independent variables were selected for the statistical experiment design as follows; Two numerical factors: Wind speed (A, m/s), Distance Ratio between turbines (B, %), and one categorical factor: turbine arrangement type (C, −). The range and level of the factors varied accordingly to the experimental design.

$$Y = f(X_1, X_2 \ldots X_n) \quad (1)$$

where Y is the experiment's response (Power Ratio), and X_n is the independent variable and named factors. The purpose of the experimental design is to optimize the response variables (Y). Identifying a fine approximation for the actual correlation between independent variables and response (Y) is necessary. The experiment was performed randomly to reduce errors and the effect of uncontrolled factors. Consequently, a

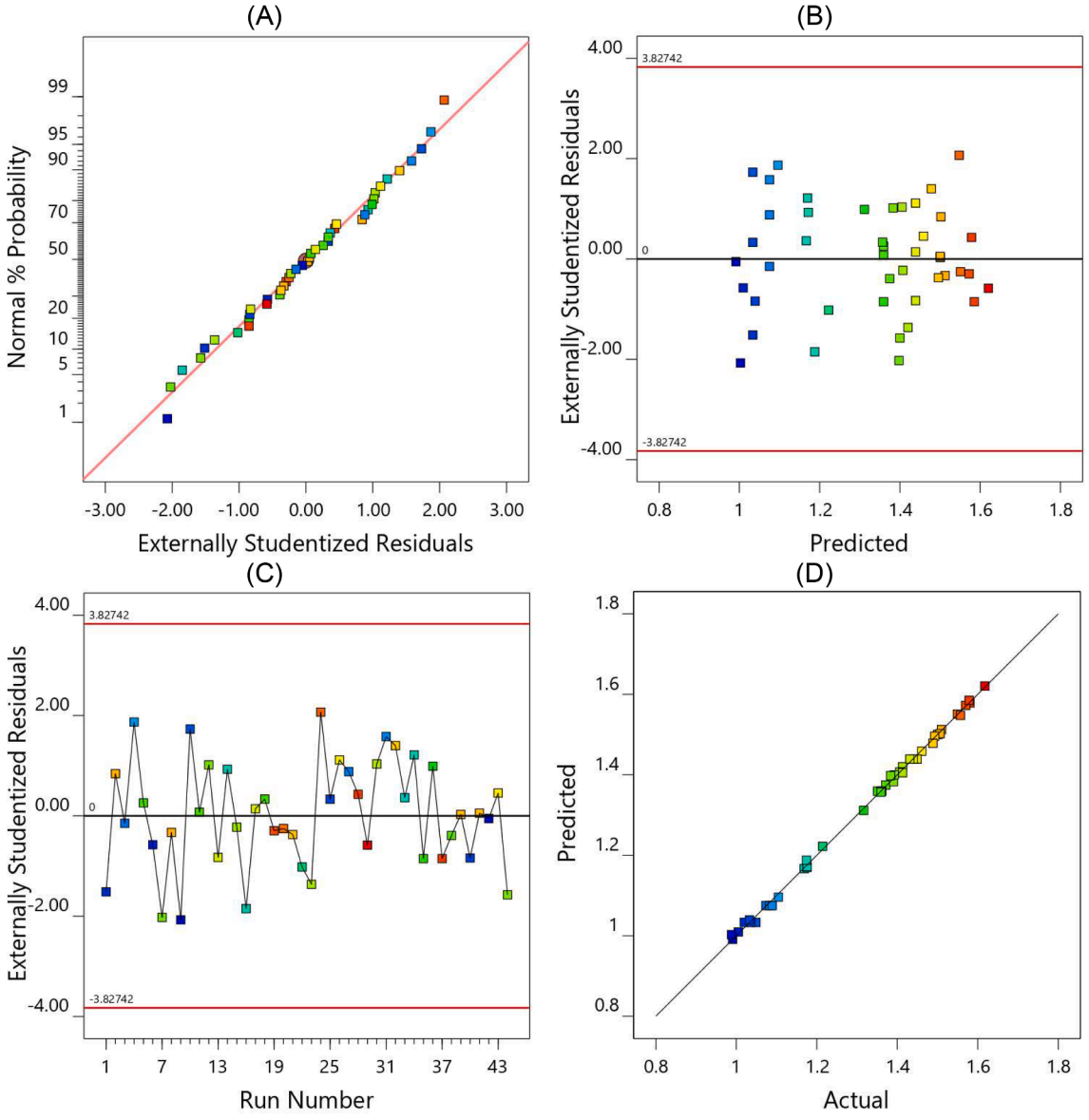

Fig. 7. The CCD Normal probability vs. Externally studentized residuals (A), Externally studentized residuals vs. Predicted value of power ratio (B) and Number of runs (C), and Predicted power ratio vs. actual power ratio.

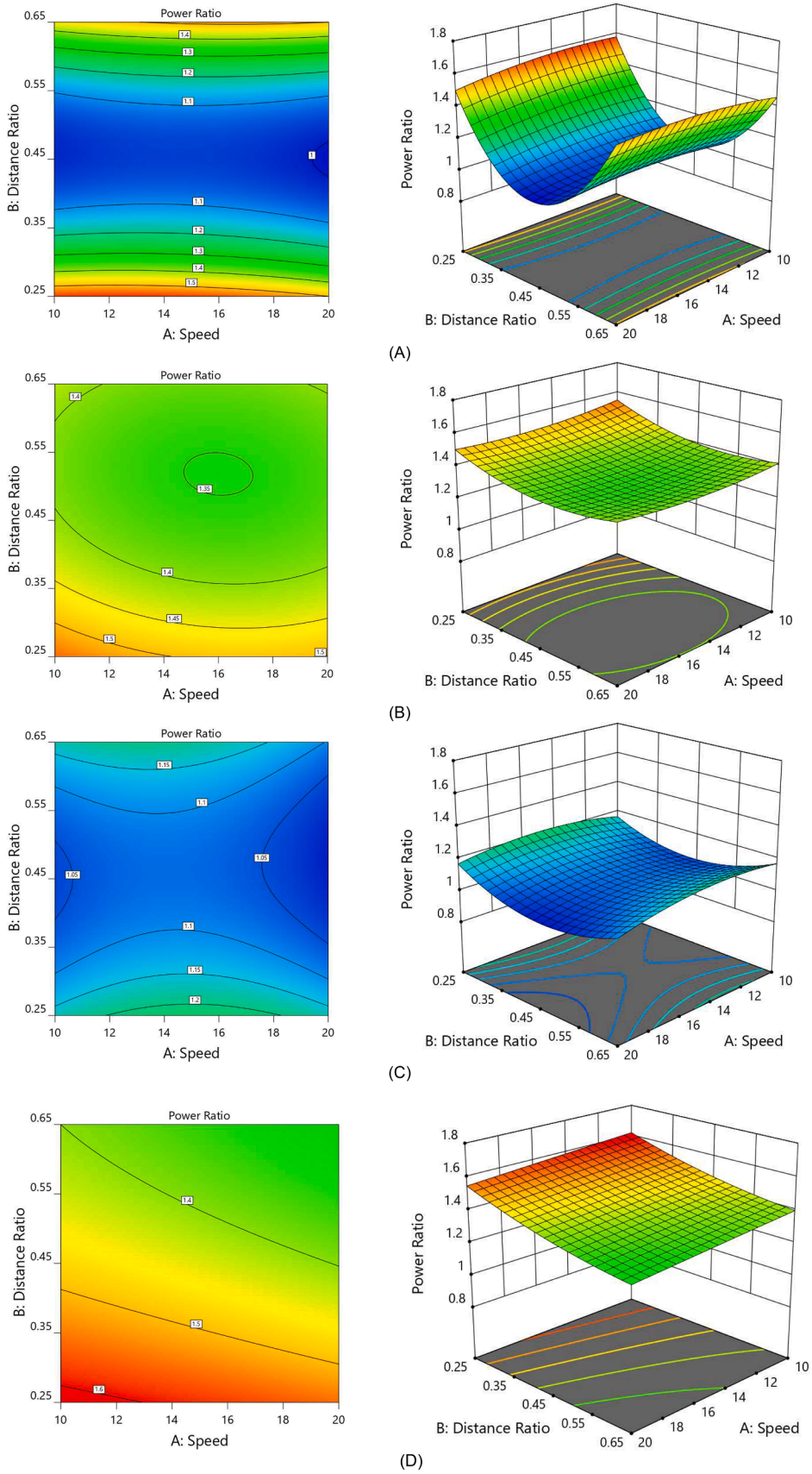

Fig. 8. The response surface and contour plots of power ratio as a function of wind speed (m/s) and distance ratio in different turbine rotor types of CO-SB (A), CO-BB (B), CR-SB (C), and CR-BB (D).

central composite design (CCD) was presented to improve the power ratio increment in the suitable distance ratio of turbine rotors. In the statistical study, the response with a related set variable was modeled to optimize the process status for the desired response. ANOVA was employed to compute the statistical parameters with the support of response surface methods. The number of runs required to quantify the effects of two numerical factors and one categorical factor is given by [27,28]:

$$N = n_t\,(2^n + 2n + n_c) = 4 \times (2^2 + 2 \times 2 + 3) = 44 \quad (2)$$

where N is the total number of required runs, n_t is the quantity of categorical factors n is the number of numerical factors and n_c is the number of replications.

2.6. Data analysis

The mathematical analysis can sometimes evaluate the practical domain after matching the results with the data. The use of ANOVA is another effective technique for evaluating model quality [29]. The basic concept of ANOVA is to compare the change caused by the variation of the variable quantity with the change caused by accidental errors inherent in the resulted errors as a consequence of the response

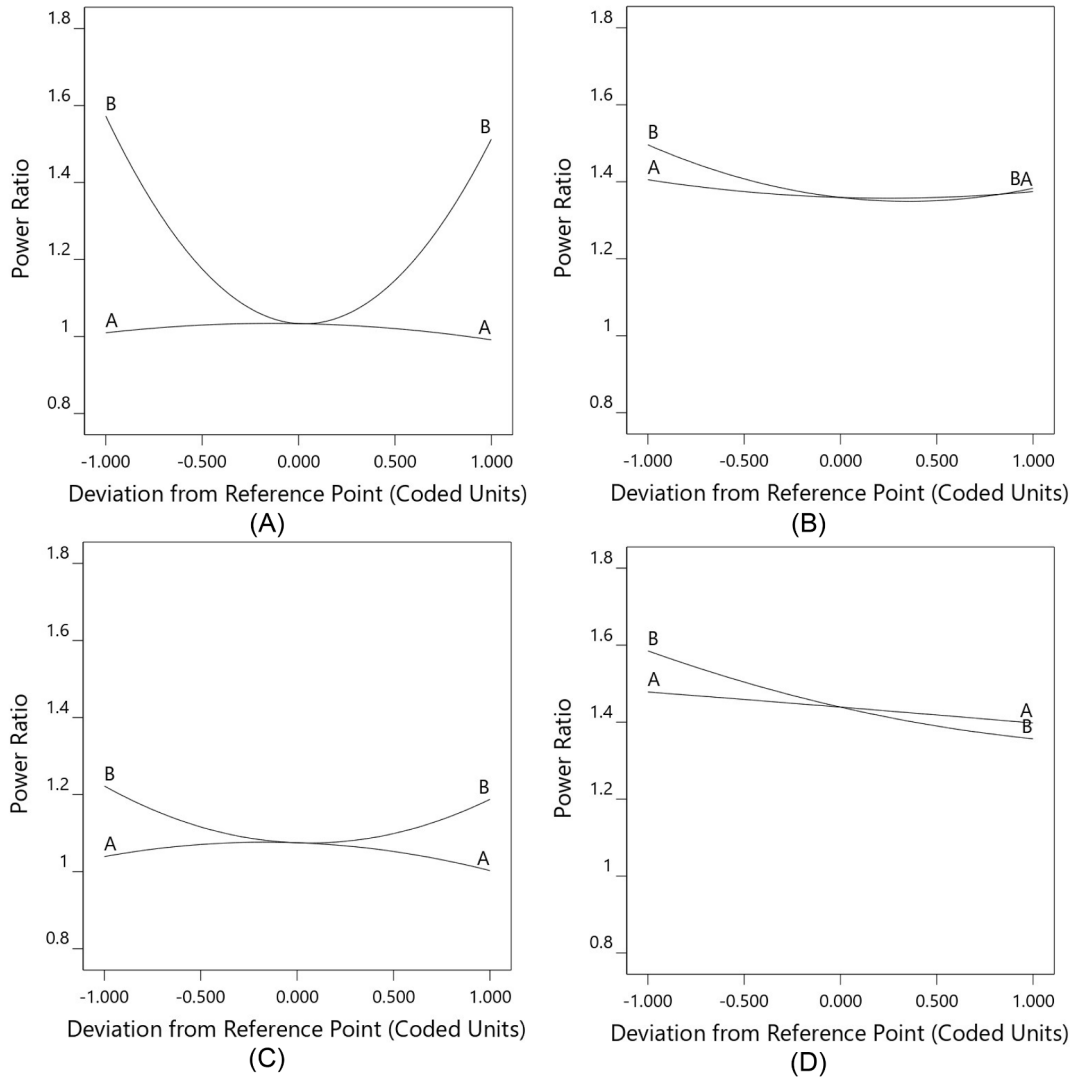

Fig. 9. Deviation curves for power ratio responses with coded factors for CO-SB (A), CO-BB (B), CR-SB (C), and CR-BB (D) types of turbines.

Table 2
Optimum values for designed parameters and response.

Parameter	Goal	Lower	Upper	Optimum Values
Wind Speed (m/s)	In range	10	20	20
Distance Ratio	In range	0.25	0.65	0.25
Turbine Type	In range	CO-SB, CO-BB, CR-SB, CR-BB		CR-BB
Power Ratio	Maximum	0.988	1.618	1.548
Power (mW)	Maximum	1751.77	12938.3	12672.5
Desirability	–	0	1	0.961

calculations.

Design Expert 12.0 software used for statistical analysis of experimental data and estimate the coefficient of the model. This software used a one-way ANOVA to estimate the coefficients of the designed model. ANOVA was used to consider the adequacy and fitness of responses to variables based on designed model functions. The model with a P-Value less than 0.05 is deemed to be significant. Then validation of the model was calculated by the coefficient of determination (R^2), and its statistic was significantly checked by F Value. The lack of fit test was applied to check the residual and pure errors at replicated points. The predicted residual sum of squares employed as an index to validate the designed model is fitted to the points [30]. Functions and equations applied in data analysis were the same as used in Prakash Maran [31] and Pashaei [32] study.

3. Result and discussion

3.1. Measuring output power

Two DC motors were used to measure the output power of the rotors installed inside the duct in different arrangements of rotors. Motors were tested in the same inlet wind speed, wind load, and ambient conditions to verify the same output. It was found that all motors had the same performance. Each DC-generator's output voltage and power are shown separately as a turbine rotational speed (rpm) function in Fig. 6. The maximum voltage reached 2.2 mV while the output power was limited to 280 mW at about 3800 rpm. The outcome of voltage and power are the same for each of the two turbines then there is no difference between the DC-motor used in the front or rear rotor of the turbine.

3.2. Comparison of the output power of dual-rotor wind turbines

The optimum distance between two rotors and the impact of the rotation direction of two rotors on the output power was considered. Abbreviations were applied to simplify the names and arrangements of the rotors. The large rotors were indicated by the letter B, while the smaller rotors were denoted by the letter S. Naming the combination of the turbines from the first rotor done from the left, for example, the BS shows the big rotor at the front and the small rotor at the end. Also, CO Abbreviation was used for Co-Rotating rotation of the turbines, and CR was used for Counter-Rotating rotation of the turbines. For example, the SB-CR represents a dual-rotor turbine with a small rotor at the front and a large rotor at the rear, and the two rotors rotate in opposite directions.

3.2.1. Effect of distance between turbines on output power

The RSM was employed to investigate the effect of independent variables on output power ratio. In this study, two critical numerical

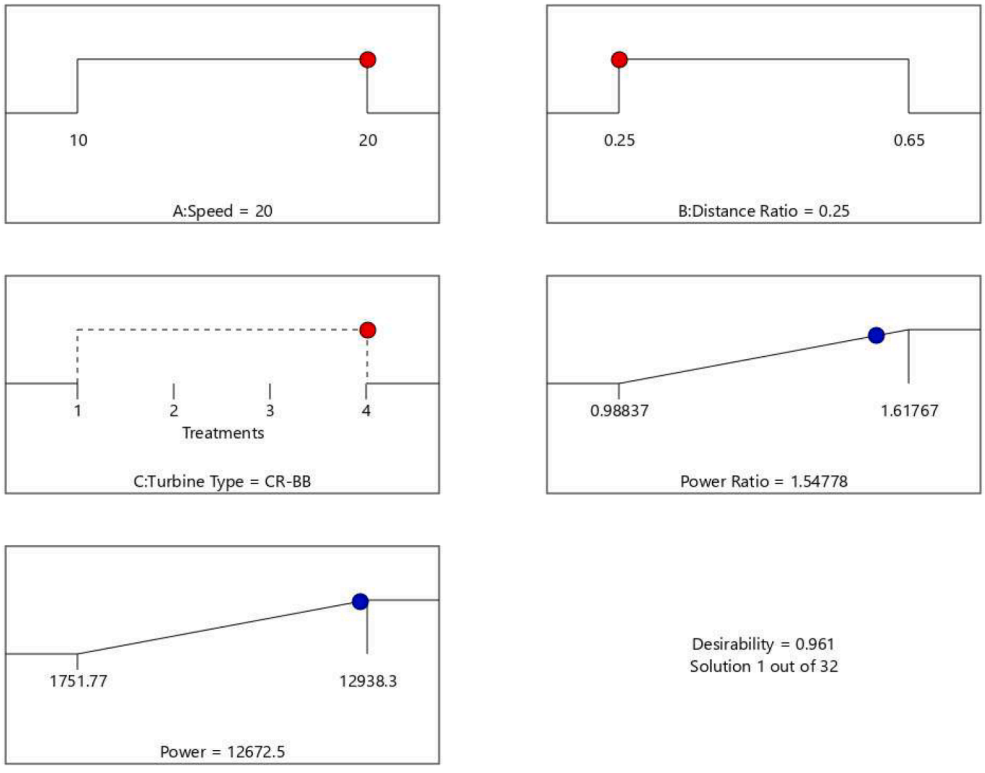

Fig. 10. Desirability ramp for optimization of parameters for maximum Power ratio and power.

parameters, Speed (A), Distance Ratio (B), and one categorical parameter turbine arrangement type (C) investigated as independent variables, and the power ratio (Y) chose as a dependent variable (response). The designed model includes four categorial parameters with eight test points and three replications for each category; then, 44 experimental tests are included in this study. Table A2 is shown the experimental design variables and experimental responses for the designed model.

The experimental results were studied to provide an appropriate regression model. "Design Expert 12" software was used to analyze CCD responses and results for the ANOVA and a sketch of the response surface model. The best significant models based on the different type of turbines, as suggested by the software, are as follow:

$$\text{CO-SB: Power Ratio (Y)} = 3.61 + 24.24 \times 10^{-3} \times A - 12.05 \times B + 29.89 \times 10^{-3} \times AB - 1.32 \times 10^{-3} \times A^2 + 12.73 \times B^2 \quad (3)$$

$$\text{CO-BB: Power Ratio (Y)} = 2.28 - 43.99 \times 10^{-3} \times A - 2.22 \times B + 9.07 \times 10^{-3} \times AB + 1.23 \times 10^{-3} \times A^2 + 2.01 \times B^2 \quad (4)$$

$$\text{CR-SB: Power Ratio (Y)} = 1.21 + 69.96 \times 10^{-3} \times A - 2.72 \times B - 19.67 \times 10^{-3} \times AB - 2.16 \times 10^{-3} \times A^2 + 3.25 \times B^2 \quad (5)$$

$$\text{CR-BB: Power Ratio (Y)} = 1.94 - 5.14 \times 10^{-3} \times A - 1.23 \times B - 3.88 \times AB - 3.89 \times 10^{-5} \times A^2 + 0.8 \times B^2 \quad (6)$$

where A & B are coded values for wind speed and distance ratio, AB is interaction terms, and A^2 and B^2 are squared terms of studied parameters. In these equations, the positive sign presented the increasing effect of each factor on power ratio (response), while the negative sign shown a decreasing impact of factors on the power ratio. Table A3 is shown the ANOVA and statistical parameters for the power ratio. If the model presents a significant regression and a non-significant lack of fit, then experimental data will fit the model well. The designed model and its factors have a significant result on the response because of the large F-value. The Model F-value of 617.54 implies that the model is significant. According to the calculated p-value, there is only a 0.01% chance that this large F-value could occur due to noise. The low error probability value shows that the designed model can statistically represent a suitable estimate of experiment data. P-values less than 0.05 indicate model terms are significant, while values lower than 0.001 shown the variable is highly significant in model response, and values higher than 0.1 represent that the model or its factors are insignificant [32,33]. The Lack of Fit F-value of 1.36 implies that the Lack of Fit is insignificant relative to the pure error. A non-significant lack of fit is good, and we want the model to fit well to predicted data [25,34].

The R^2 value (coefficient determination) presented the variance of the data in the designed model. R^2 is the proportion of the variance in the dependent variable (response) that is predictable from the independent variable (predictors). R^2 closer to 1 indicates the suitable fit of the model to data. The R^2 value is shown in Table A4; the values more than 0.99 show that the model fits data with high accuracy, and the designed model cannot predict only 0.14% of data. A high adjusted R^2 value shows the developed model is adequate to predict power ratio in different independent variables. The Predicted R^2 of 0.9910 is in reasonable agreement with the Adjusted R^2 of 0.9970; i.e., the difference is less than 0.2. The adequate precision of this correlation for power ratio is 78.91 (adeq. precision > 4), which shows the model noise ratio is placed in a reasonable range. An adequate precision greater than 4 is desirable, and this model can be used to navigate the design space. Also, lower values for standard deviation (0.0108) and coefficient of variance (0.8170) showed better model accuracy and validity.

The important section to investigate the data analysis of the experiment was the adequacy of the designed model. The normal probability vs. studentized residual plot for the output power ratio is shown in Fig. 7 (A). The plot shows that there is neither a need to respond to transformation nor an obvious problem with normality. Fig. 7(B) presented the externally studentized residual vs. predicted power ratio. It denoted that the data variance is constant for the measured response, and transportation of measured responses is not required. Fig. 7(C) is shown the externally residual plot for power ratio vs. the run number of designed experiments. It seems there is no outlier in the residual plot, and all of the residuals are constantly scattered along with the different runs. The predicted vs. actual experiment data plot for power ratio is presented in Fig. 7(D). The difference in the color of points is shown in the prediction results for low and high power ratio values. It is clear from this figure that points are generally placed on a straight line, and the actual and predicted values are close to each other for all responses. Thus, the ANOVA analysis results show that the designed model was fitted to experimental data. The offered model is valid for predicting the ducted wind turbines power ratio.

Evaluation of the correlative relationship between the designed parameters of wind speed and distance ratio vs. the power ratio for dual rotor ducted wind turbines is shown in Fig. 8 by employing contours and 3D plots of RSM. Fig. 8 presents these plots for power ratio (response) as a function of wind speed (m/s) and distance ratio while the turbine types changed in four rotor arrangements. From the contour and 3D plots of power ratio in Fig. 8(A), it was found that distance ratio influence on power ratio for the CO-SB turbine type. In low values and high values for distance ratio, the maximized value of power ratio is extracted. Placing a small wind rotor in the front of a bigger one gets enough time and space for wind flow to recover before arriving at the big rotor. Therefore, after a decrease in power ratio in the mid-range of distance ratio, an increase occurred in the high-range distance ratio. Fig. 8(B) is shown the counter and 3D plots of power ratio for CO-BB wind turbine type. It is clear that compared to the previous case, wind energy harvest is more uniform in different distance ratios, while with decreasing the distance ratio, the power ratio is increased. Fig. 8(C) is presented the counter-plot and 3D surface of power ratio for the CR-SB wind turbine type. The 3D surface pattern is similar to the CO-SB turbine type, but harvested wind energy is lower than the previous state. The similarity of the plotted responsive surfaces for CO-SB and CR-SB indicates the similar effect of placing a small rotor in front of a larger rotor in the extracted power ratio of ducted wind turbines.

The counter-plot and 3D response surface of the power ratio for CR-BB wind turbine type are displayed in Fig. 8(D). This plot indicates that the level of harvested wind energy is higher than other types of turbines, and any reduction in distance ratio causes the output power ratio to increase. The counterplot and 3D response surface displayed in Fig. 8(A, B, C, and D) showed a significant relationship between power and distance ratios. The interaction between wind speed and power ratio observed that the increment in wind speed was not affected by the power ratio. In other means, it is clear that the distance ratio changes have a more significant effect on the output power ratio than the wind speed changes, and a higher power ratio was observed at lower distance ratios. In all cases, by selecting the appropriate distance ratio between the two rotors, the output power ratio can be increased up to 20% in turbines.

In designed models with the RSM technique, deviation plots discovered the influence of model parameters on the derived response by revealing the effect of changes in each parameter on the response as it moves from the reference point, each parameter is in zero coded levels, while other parameters set to be constant at the reference point value. The perturbation plot to analyze the effect of model parameters (wind speed and distance ratio) at the center point (0) is shown in Fig. 9. It is indicated from Fig. 9(A & C) for turbines with a small rotor in front of the turbine; the power ratio decreases in mid-range of distance ratio between two rotors while the changes related to increasing wind speed is negligible. For turbines with two big rotors, as shown in Fig. 9(B & D), the power ratio decreases when the distance ratio between two rotors increases and an increase of wind speed. In comparison, the reduction rate of power ratio for distance ratio was more than wind speed.

Table 3
Comparison of Power Ratio between experimental and RSM results for the optimum condition.

No	Optimum Design Parameters	Power Ratio		
		Experiment Result	RSM Result	Error (%)
1	V = 20 m/s DR = 0.25 Turbine = CR-BB	1.53	1.55	0.6

3.3. Optimum conditions for maximum power

The goal of investigating the optimal power ratio is to determine the designed parameters, giving the power's optimal operation. The designed parameters and model response required details in the optimization process are shown in Table 2. As shown in Table 2, two responses (power and power ratio) are considered in the optimization. The input parameters were set to be in a specified range, while the responses were set to achieve maximum value. Using these conditions, the maximum achieved power ratio and the ducted wind turbine's power were 1.548 and 12672.5 mW, respectively; (Table 2 & Fig. 9) at a wind speed of 20 m/s, distance ratio of 0.25, and CR-BB turbine type.

Fig. 10 represented that the output results of the designed model are close to the maximum expectation set for the model. The desirability value is presented as a variable from 0 to 1, showing the output's proximity to the desired output. Then it indicates how designed factors are optimally set to assure the responses, and the desirability value near 1 (0.961) is a good result for optimization. The RSM model results are compared with experimental results, as shown in Table 3, to confirm optimum conditions for the designed parameters. According to the confirmation test, it is observed that the reported error (0.6%) between the actual and predicted power ratio is shown a little difference, which shows a good matching between the designed RSM model and experimental tests.

Dual-rotor wind turbines with various rotor types were utilized in this research. Table 4 shows comparisons of optimized parameters and responses to those in previous researchers' studies. The present research found that the power ratio for twin rotor wind turbines was more incredible than the previous finding. This study shows that the duct helps to increase the output power ratio in dual-rotor wind turbines. In comparison, the RSM as an optimization method can optimize the performance of dual-rotor wind turbines in DWT's. Previous researchers recognize different strategies to improve the performance of dual-rotor wind turbines in specific ways. The increase of power for dual rotor turbines was higher in comparison to single rotor wind turbines. At the same time, there is no defined method to compare the performance of the different types of dual-rotor wind turbines in ducts. This study designed the RSM model for different types of dual-rotor wind turbines to perform these targets.

Table 4
Comparison between the present study and previous work results.

No.	References	Optimum Parameters	Maximum Power Ratio
1	Shen et al. [35]	Wind speed: 5–20 m/s Distance Ratio: 0.1–0.8 Turbine Radius Turbine Type: CR-BB	43.5%
2	Rosenberg et al. [36]	Wind speed: 8 m/s Distance Ratio: 0.2 Turbine Radius Turbine Type: CR-SB	7%
3	Agung and Huda [37]	Wind speed: 4.2 m/s Distance Ratio: 0.44 Turbine Radius Turbine Type: CR-SB	24%
4	Wang et al. [38]	Wind speed: 6.5 m/s Distance Ratio: 0.25D Turbine Type: CR-SB, CO-SB	7.2%
5	Didane et al. [39]	Wind speed: 5 m/s Distance Ratio: 0.16 m Turbine Type: CR-BB	40%
6	Present Study	Wind speed: 20 m/s Distance Ratio: 0.25 Turbine Type: CR-BB	55%

4. Conclusion

In this research, we considered the effect of using two different types of rotors for DRWT's and main parameters like distance ratio between rotors and wind speed in the throat section of the duct on the produced power ratio in ducted wind turbines. Input parameters optimized by using the simulation–optimization RSM analysis method to maximize the power ratio. Optimization of variables done by CCD of RSM techniques to develop the model and the standard deviation of the model was 0.01. The reported P-value of the model for turbine type, distance ratio between two rotors, and wind speed obtained less than 0.05 showed a significant effect of parameters on the designed model. RSM presented the interaction between investigated factors like turbine type, distance ratio between rotors, and wind speed. Validation of the proposed model using regression analysis of parameters shown that we can use this model to determine input parameters to reach maximum extracted power. This model offered a reliable tool for evaluating the design parameters and performance of DRWT's. Optimized conditions

for DRWT installed in the throat section of a duct are a counter-rotating dual rotor wind turbine with two big rotors, a 0.25 distance ratio between two rotors related to duct throat section diameter, and 20 m/s for enhanced wind speed at the duct throat section. At this condition experimental performance of DRWT shown an increase of 55% in produced power compared to the single rotor wind turbine. RSM is helpful to optimize the extracted power of DRWT's to achieve specific experimental goals. RSM with high prediction efficiency is valid in predicting the suitable performance of DRWT's; thus, the difficulty of repetitive practical experiments and its related costs are omitted, and rapid decision making for designing application of DRWT's developed.

CRediT authorship contribution statement

Javad Taghinezhad: Conceptualization, Methodology, Software, Experimental Tests, Writing – original draft. **Reza Alimardani:** Visualization, Supervision, Writing - review & editing. **Mehran Masdari:** Experimental Tests, Software, Writing - review & editing, Supervision, Methodology. **Esmail Mahmoodi:** Writing - review & editing.

Declaration of Competing Interest

The authors declare that they have no known competing financial interests or personal relationships that could have appeared to influence the work reported in this paper.

Appendix A. Tables

Table A1
Blade characterization as a function of the blade radius.

α (deg)	r/R	c/R
28.6	0.15	2.67
21.4	0.2	2.37
16.5	0.25	2.08
13.1	0.3	1.83
10.7	0.35	1.61
9	0.4	1.45
7.8	0.45	1.31
7	0.5	1.19
6.4	0.55	1.09
6.1	0.6	1.01
5.9	0.65	0.93
5.8	0.7	0.87
5.8	0.75	0.81
5.9	0.8	0.77
6.1	0.85	0.72
6.4	0.9	0.68
6.7	0.95	0.65
7	1	0.61

Table A2
CCD experimental design variables and practical responses.

Run	Speed (m/s)	Distance Ratio	Turbine Type	Power Ration	Output Power (mW)	Run	Speed (m/s)	Distance Ratio	Turbine Type	Power Ration	Output Power (mW)
1	15	0.45	CO-SB	1.01978	4008.9	**23**	10	0.65	CO-BB	1.41335	2428.47
2	20	0.25	CO-BB	1.50636	12216.3	**24**	20	0.25	CR-BB	1.55717	12938.3
3	15	0.45	CR-SB	1.07362	4041.4	**25**	15	0.45	CO-SB	1.03653	4015.2
4	20	0.65	CR-SB	1.10465	8183.57	**26**	15	0.45	CR-BB	1.44925	5402.26
5	15	0.45	CO-BB	1.36163	6004.07	**27**	15	0.45	CR-SB	1.08323	4059.3
6	10	0.45	CO-SB	1.00509	1751.77	**28**	10	0.25	CO-SB	1.58073	2789.9
7	20	0.45	CR-BB	1.38347	11000.6	**29**	10	0.25	CR-BB	1.61767	2854.3
8	15	0.65	CO-SB	1.50993	5733.26	**30**	10	0.45	CO-BB	1.413	2497.58
9	20	0.45	CR-SB	0.98837	7225.27	**31**	15	0.45	CR-SB	1.08915	4066.1
10	15	0.45	CO-SB	1.04867	3998.3	**32**	10	0.45	CR-BB	1.48863	2594.53
11	15	0.45	CO-BB	1.35987	5095.98	**33**	10	0.25	CR-SB	1.16866	2036.85
12	15	0.65	CO-BB	1.39066	5211.37	**34**	20	0.25	CR-SB	1.17572	8605.26
13	15	0.45	CR-BB	1.43124	5391.32	**35**	15	0.45	CO-BB	1.35124	5089.98
14	10	0.65	CR-SB	1.17627	2050.13	**36**	20	0.65	CR-BB	1.3165	10468.1
15	20	0.65	CO-BB	1.40624	11022.6	**37**	15	0.25	CR-BB	1.57866	5915.8
16	15	0.65	CR-SB	1.17459	4401.67	**38**	20	0.45	CO-BB	1.3715	10905.4
17	15	0.45	CR-BB	1.44032	5397.45	**39**	20	0.25	CO-SB	1.5008	10603.3
18	15	0.65	CR-BB	1.35937	5206.54	**40**	10	0.45	CR-SB	1.03285	1800.15
19	15	0.25	CO-SB	1.57025	5959.3	**41**	20	0.65	CO-SB	1.50065	9991.3
20	10	0.25	CO-BB	1.54974	2701.04	**42**	20	0.45	CO-SB	0.99098	7882.15
21	15	0.25	CO-BB	1.49305	5595.04	**43**	10	0.65	CO-SB	1.46101	2846.4
22	15	0.25	CR-SB	1.21458	4551.5	**44**	10	0.65	CR-BB	1.39252	2427.02

Table A3
ANOVA table for the power ratio.

Source	Sum of Squares	df	Mean Square	F-value	p-value	
Model	1.66	23	0.0720	617.54	<0.0001	significant
A-Speed	0.0103	1	0.0103	88.35	<0.0001	
B-Distance Ratio	0.0712	1	0.0712	611.35	<0.0001	
C-Turbine Type	0.7758	3	0.2586	2218.89	<0.0001	
AB	0.0002	1	0.0002	2.04	01689	
AC	0.0033	3	0.0011	9.51	0.0004	
BC	0.0333	3	0.0111	95.30	<0.0001	
A^2	0.0021	1	0.0021	17.77	0.0004	
B^2	0.3576	1	0.3576	3068.40	<0.0001	
ABC	0.0053	3	0.0018	15.08	<0.0001	
A^2C	0.0104	3	0.0035	29.85	<0.0001	
B^2C	0.3608	3	0.1203	1032.02	<0.0001	
Residual	0.0023	20	0.0001			
Lack of Fit	0.0016	12	0.0001	1.36	0.3400	not significant
Pure Error	0.0008	8	0.0001			
Correlation Total	1.66	43				

Table A4
ANOVA for Response Surface Designed Model.

Factors	%
R^2	0.9986
Adjusted R^2	0.9970
Predicted R^2	0.9910
Adeq Precision	78.9147
Std. Dev.	0.0108
Mean	1.32
C.V. %	0.8170

References

[1] Allaei D, Andreopoulos Y. INVELOX: a new concept in wind energy harvesting. In: ASME 2013 7th International Conference on Energy Sustainability; 2013. p. 1–5.
[2] Allaei D, Andreopoulos Y. INVELOX: Description of a new concept in wind power and its performance evaluation. Energy 2014;69:336–44. https://doi.org/10.1016/j.energy.2014.03.021.
[3] Allaei D. Using CFD to Predict the Performance of Innovative Wind Power Generators. In: Proceedings of the 2012 COMCOL Conference; 2012. p. 2–3. https://doi.org/10.1111/1467-9655.12497.
[4] Allaei D, Tarnowski D, Andreopoulos Y. INVELOX with multiple wind turbine generator systems. Energy 2015;93:1030–40. https://doi.org/10.1016/j.energy.2015.09.076.
[5] Gavade AA, Mulla AS, Ransing AM, Sane NM. Design and manufacturing of INVELOX to generate Wind power using nonconventional energy sources. Int J Adv Res Sci Eng 2018:588–92.
[6] Al-Bahadly I. Wind Turbines. 1st ed. InTech; 2011.
[7] Bontempo R, Manna M. Diffuser augmented wind turbines: review and assessment of theoretical models. Appl Energy 2020;280:115867. https://doi.org/10.1016/j.apenergy.2020.115867.
[8] Saeed M, Kim MH. Aerodynamic performance analysis of an airborne wind turbine system with NREL Phase IV rotor. Energy Convers Manage 2017;134:278–89. https://doi.org/10.1016/j.enconman.2016.12.021.
[9] Hosseini SR, Ganji DD. A novel design of nozzle-diffuser to enhance performance of INVELOX wind turbine. Energy 2020;198:117082. https://doi.org/10.1016/j.energy.2020.117082.
[10] Bontempo R, Manna M. Effects of the duct thrust on the performance of ducted wind turbines. Energy 2016;99:274–87. https://doi.org/10.1016/j.energy.2016.01.025.
[11] Taghinezhad J, Alimardani R, Mosazadeh H, Masdari M. Ducted wind turbines a review. Int J Future Revol Comput Sci Commun Eng 2019;5:19–25.
[12] Khalefa MZ, Abd Alkarim SF, Salih RS. In: Optimized manufacturing of the small dual wind turbine used to generate electricity in central Iraq areas. IOP Publishing; 2020. https://doi.org/10.1088/1757-899X/765/1/012023.
[13] Walia A, Mehta P, Guleria S, Shirkot CK. Improvement for enhanced xylanase production by Cellulosimicrobium cellulans CKMX1 using central composite design of response surface methodology. 3 Biotech 2015;5:1053–66. https://doi.org/10.1007/s13205-015-0309-2.
[14] Berkani M, Bouchareb MK, Bouhelassa M, Kadmi Y. Photocatalytic degradation of industrial dye in semi-pilot scale prototype solar photoreactor: optimization and modeling using ANN and RSM based on box-wilson approach. Top Catal 2020;63:964–75. https://doi.org/10.1007/s11244-020-01320-0.
[15] Srivastava M, Maheshwari S, Kundra T, Rathee S. Multi-response optimization of fused deposition modelling process parameters of ABS using Response Surface Methodology (RSM)-based desirability analysis. Mater Today: Proc 2017;4:1972–7. https://doi.org/10.1016/j.matpr.2017.02.043.
[16] Tabatabaeikia S, Ghazali NNBN, Chong WT, Shahizare B, Izadyar N, Esmaeilzadeh A, et al. Computational and experimental optimization of the exhaust air energy recovery wind turbine generator. Energy Convers Manage 2016;126:862–74. https://doi.org/10.1016/j.enconman.2016.08.039.
[17] Hasanien HM, Muyeen SM. Design optimization of controller parameters used in variable speed wind energy conversion system by genetic algorithms. IEEE Trans Sustainable Energy 2012;3:200–8. https://doi.org/10.1109/TSTE.2012.2182784.
[18] Toft HS, Svenningsen L, Moser W, Sørensen JD, Thøgersen ML. Assessment of wind turbine structural integrity using response surface methodology. Eng Struct 2016;106:471–83. https://doi.org/10.1016/j.engstruct.2015.10.043.
[19] Fabrication WNK. Testing and Performance Enhancement of a Small Scale Tidal Current Turbine. Master Dissertation. University of Malaya Kuala Lumpur; 2016.
[20] Taghinezhad J, Mahmoodi E, Masdari M, Alimardani R. Simulation and optimization of ducted wind turbines using the response surface methodology and analytical hierarchical process. In: 7th Iran Wind Energy Conference (IWEC2021). IEEE; 2021. p. 1–6. https://doi.org/10.1109/IWEC52400.2021.9466971.
[21] Shi L, Feng F, Guo W, Li Y. Research and development of a small-scale icing wind tunnel test system for blade airfoil icing characteristics. Int J Rotating Mach 2021;2021:1–12. https://doi.org/10.1155/2021/5598859.
[22] Zanoun ES. Flow characteristics in low-speed wind tunnel contractions: simulation and testing. Alexandria Eng J 2018;57:2265–77. https://doi.org/10.1016/j.aej.2017.08.024.
[23] Pape M, Kazerani M. An offshore wind farm with DC collection system featuring differential power processing. IEEE Trans Energy Convers 2020;35:222–36. https://doi.org/10.1109/TEC.2019.2951331.
[24] Javaherchi T, Stelzenmuller N, Aliseda A. Experimental and numerical analysis of the performance and wake of a scale-model horizontal axis marine hydrokinetic turbine. J Renewable Sustainable Energy 2017;9:1–23. https://doi.org/10.1063/1.4999600.
[25] Behera SK, Meena H, Chakraborty S, Meikap BC. Application of response surface methodology (RSM) for optimization of leaching parameters for ash reduction from low-grade coal. Int J Mining Sci Technol 2018;28:621–9. https://doi.org/10.1016/j.ijmst.2018.04.014.
[26] Leonzio G. Fluid dynamic study of anaerobic digester: optimization of mixing and geometric configuration by using response surface methodology and factorial

design. Renewable Energy 2019;136:769–80. https://doi.org/10.1016/j.renene.2018.12.115.
[27] Qader BS, Supeni EE, Ariffin MKA, Talib ARA. RSM approach for modeling and optimization of designing parameters for inclined fins of solar air heater. Renewable Energy 2019;136:48–68. https://doi.org/10.1016/j.renene.2018.12.099.
[28] Rahmannezhad J, Mirbozorgi SA. CFD analysis and RSM-based design optimization of novel grooved micromixers with obstructions. Int J Heat Mass Transfer 2019;140:483–97. https://doi.org/10.1016/j.ijheatmasstransfer.2019.05.107.
[29] Chen WH, Wang JS, Chang MH, Mutuku JK, Hoang AT. Efficiency improvement of a vertical-axis wind turbine using a deflector optimized by Taguchi approach with modified additive method. Energy Convers Manage 2021;245:114609. https://doi.org/10.1016/j.enconman.2021.114609.
[30] Ghaemi A, Mashhadimoslem H, Zohourian IP. NiO and MgO/activated carbon as an efficient CO2 adsorbent: characterization, modeling, and optimization. Int J Environ Sci Technol 2021. https://doi.org/10.1007/s13762-021-03582-x.
[31] Prakash Maran J, Sivakumar V, Thirugnanasambandham K, Sridhar R. Artificial neural network and response surface methodology modeling in mass transfer parameters predictions during osmotic dehydration of Carica papaya L. Alexandria Eng J 2013;52:507–16. https://doi.org/10.1016/j.aej.2013.06.007.
[32] Pashaei H, Ghaemi A, Nasiri M, Karami B. Experimental modeling and optimization of CO2 absorption into piperazine solutions using RSM-CCD methodology. ACS Omega 2020;5:8432–48. https://doi.org/10.1021/acsomega.9b03363.
[33] Khodaei B, Sobati MA, Shahhosseini S. Optimization of ultrasound-assisted oxidative desulfurization of high sulfur kerosene using response surface methodology (RSM). Clean Technol Environ Policy 2016;18:2677–89. https://doi.org/10.1007/s10098-016-1186-z.
[34] Tan YH, Abdullah MO, Nolasco-Hipolito C, Ahmad Zauzi NS. Application of RSM and Taguchi methods for optimizing the transesterification of waste cooking oil catalyzed by solid ostrich and chicken-eggshell derived CaO. Renewable Energy 2017;114:437–47. https://doi.org/10.1016/j.renene.2017.07.024.
[35] Shen WZ, Zakkam VAK, Sørensen JN, Appa K. Analysis of counter-rotating wind turbines. J Phys Conf Ser 2007;75:1–9. https://doi.org/10.1088/1742-6596/75/1/012003.
[36] Rosenberg A, Selvaraj S, Sharma A. A novel dual-rotor turbine for increased wind energy capture. J Phys Conf Ser 2014;524:1–10. https://doi.org/10.1088/1742-6596/524/1/012078.
[37] Agung Bramantya M, Huda L. An experimental study on the mechanics power of counter rotating wind turbines model related with axial distance between two rotors. In: . Proceedings - 2016 6th International Annual Engineering Seminar, InAES 2016, Yogyakarta, Indonesia; 2017. p. 212–7. https://doi.org/10.1109/INAES.2016.7821936.
[38] Wang Z, Ozbay A, Tian W, Hu H. An experimental study on the aerodynamic performances and wake characteristics of an innovative dual-rotor wind turbine. Energy 2018;147:94–109. https://doi.org/10.1016/j.energy.2018.01.020.
[39] Didane DH, Rosly N, Zulkafli MF, Shamsudin SS. Performance evaluation of a novel vertical axis wind turbine with coaxial contra-rotating concept. Renewable Energy 2018;115:353–61. https://doi.org/10.1016/j.renene.2017.08.070.